Journal of Hazardous Materials 170 (2009) 203–209

Contents lists available at ScienceDirect

Journal of Hazardous Materials

journal homepage: www.elsevier.com/locate/jhazmat

Autohydrogenotrophic denitrification of drinking water using a polyvinyl chloride hollow fiber membrane biofilm reactor

Yanhao Zhang [a,b], Fohua Zhong [a], Siqing Xia [a,*], Xuejiang Wang [a], Jixiang Li [a]

[a] State Key Laboratory of Pollution Control and Resource Reuse, College of Environmental Science and Engineering, Tongji University, Shanghai 200092, China
[b] College of Municipal and Environmental Engineering, Shandong Jianzhu University, Jinan 250101, China

ARTICLE INFO

Article history:
Received 6 January 2009
Received in revised form 13 April 2009
Accepted 27 April 2009
Available online 5 May 2009

Keywords:
Autohydrogenotrohpic denitrification
Membrane biofilm reactor
Polyvinyl chloride hollow fiber
Microbial community structures

ABSTRACT

A hollow fiber membrane biofilm reactor (MBfR) using polyvinyl chloride (PVC) hollow fiber was evaluated in removing nitrate form contaminated drinking water. During a 279-day operation period, the denitrification rate increased gradually with the increase of influent nitrate loading. The denitrification rate reached a maximum value of 414.72 g N/m^3 d (1.50 g N/m^2 d) at an influent NO_3^-–N concentration of 10 mg/L and a hydraulic residence time of 37.5 min, and the influent nitrate was completely reduced. At the same time, the effluent quality analysis showed the headspace hydrogen content (3.0%) was lower enough to preclude having an explosive air. Under the condition of the influent nitrate surface loading of 1.04 g N/m^{2}d, over 90% removal efficiencies of the total nitrogen and nitrate were achieved at the hydrogen pressure above 0.04 MPa. The results of denaturing gel gradient electrophoresis (DGGE), 16S rDNA gene sequence analysis, and hierarchical cluster analysis showed that the microbial community structures in MBfR were of low diversity, simple and stable at mature stages; and the *beta-Proteobacteria*, including *Rhodocyclus*, *Hydrogenophaga*, and *beta-Proteobacteria* HTCC379, probably play an important role in autohydrogenotrophic denitrification.

1. Introduction

Nitrate in surface and ground water was highly concerned all over the world due to potential risks to human body via drinking nitrate-contaminated water. In general, nitrate was mainly from the usage of nitrogen fertilizers and the irrigation with domestic wastewater [1,2]. A standard of nitrate concentration of 10 mg/L in drinking water was recommended by World Health Organization (WHO) [3]. If the level of nitrate in water exceeds the standard, methemoglobinemia in infants would be occurred, as well as nitrosamines, potential carcinogens metabolites of nitrate, would be formed [4].

Among the physical–chemical technologies considered for NO_3^-–N removal are ion exchange [5], reverse osmosis [6], and electro-dialysis [7]. However, the utilities of these processes were limited due to high capital and energy costs and subsequent disposal problem of large volumes of waste brine [1]. Biological denitrification is an alternative technology, which is carried out by facultative bacteria that can use NO_3^-–N as a terminal electron acceptor for respiration under anoxic conditions. Reduction of NO_3^- to nitrogen gas proceeds in a four-step process: microorganisms reduce NO_3^- to NO_2^-, nitric (NO), nitrous oxide (N_2O), and finally to nitrogen gas (N_2). Generally, organic substrates such as methanol or ethanol were used during conventional denitrification process by heterotrophic denitrification because organic carbon concentration in drinking water was very low [8].

Recently, autotrophic denitrification processes, including sulfur-based denitrification [9–11] and hydrogen-based auotrophic denitrification [12–14], were widely studied in the remediation of groundwater and drinking water. For sulfur-based denitrification, limestone is needed to buffer the generated acidity. Moreover, denitrifcation rate is controlled by the ratio of sulfur/limestone, which makes this technology sophisticated and difficult to operate [15,16]. In contrast, using H_2 as electron donors to reduce nitrate, i.e., hydrogen-based autotrophic denitrification, was highlighted in recent years with the following advantages: (1) lower cell yield; (2) no further steps are needed to remove either carryover of added organic substrate or its derivatives; (3) the relatively low solubility of H_2, which makes it easy to remove from the product water by air stripping; (4) the low cost of H_2, i.e., it is by far the least expensive donor per electron donor supplied [14,17,18]. Even so, there are some drawbacks inhibiting its application, which include lower denitrification rates and the difficulty in dissolving sufficient quantities of H_2 into the water due to its low solubility [19]. In addition, the hazardous (explosive) nature of hydrogen during use, transportation and storage may limit the use of hydrogen in denitrification reactors.

* Corresponding author. Tel.: +86 21 65980440; fax: +86 21 65986313.
E-mail addresses: siqingxia@tongji.edu.cn, sdzyh08@hotmail.com (S. Xia).

0304-3894/$ – see front matter © 2009 Elsevier B.V. All rights reserved.
doi:10.1016/j.jhazmat.2009.04.114

Autohydrogenotrophic denitrification was extensively investigated to remove nitrate from polluted groundwater or surface water [12–14,20]. Kurt et al. [13] studied autotrophic denitrification in a cone-shaped fluidized sand-bed reactor using a mixed culture and achieved nitrate elimination rate of 552 g NO_3^-–N/m^3 d. Dries et al. [12] studied the performance of autohydrogenotrophic denitrification using a dual-column reactor. H_2 was supplied to the reactor by direct bubbling of H_2 gas in the downflow column, and the removal rate of 500 g NO_3^-–N/m^3 d was achieved at 20 °C. Due to the danger of explosive air and low hydrogen utility efficiency for the sparging methods, the bubbleless gas-permeable membrane technology has developed to a promising way to reduce nitrate, and the membrane choosing is a critical factor for this technology development. A number of researchers have studied bubbleless gas-permeable membranes, which mainly included composite membrane (e.g., sandwich structure: dense polyurethane layer sandwiched by outside layer and inner layer of polyethylene [14]), polypropylene [19], silicone-coated reinforced fiberglass fibers [21], and silicone-coated ferro-nickel slag [22]. Even so, there are some challenges to be overcome for the robust reactor development, such as capital cost of membrane fabrication.

The objective of this research was to investigate the performance of a hollow fiber membrane bioreactor using PVC fibers in autohydrogenotrophic denitrification of contaminated drinking water. In addition, the microbial community structure of the hydrogenotrophic denitrification culture was studied using denaturing gel gradient electrophoresis (DGGE), 16S rDNA gene sequence analysis, and hierarchical cluster analysis.

2. Material and method

2.1. Hollow fiber membrane and membrane biofilm reactor

The membrane is one of the key elements for hydrogen transferring and biofilm attaching for MBfR. The hollow fiber membranes are commonly used for MBfRs because the size of hollow fiber is smaller than other types of membrane but can give higher performance. The hollow fiber membrane used in this study is a PVC hollow fiber membrane (from Litree Co., Suzhou, China), which has a hydrophobic single layer structure (Fig. 1 left, SEM of membrane section) with the thick of about 325 μm, in detail, an inner diameter of 0.085 cm, an outer diameter of 0.15 cm, and pore size of 0.01 μm. Compared to the composite membrane (from Mitsubishi-Rayon) used in MBfR by Lee and Rittmann [14], i.e., a double-skinned polyethylene fiber with a dense internal polyurethane layer (1 μm) and pore size of 0.1–0.15 μm, the PVC hollow fiber membrane is economical in membrane fabrication, only a quarter of the composite membrane in price for per square meter according to the membrane surface area. In addition, both of them can maintain a long term running period without membrane replacement, and the economical comparison of their operation and replacement period will be researched in future research.

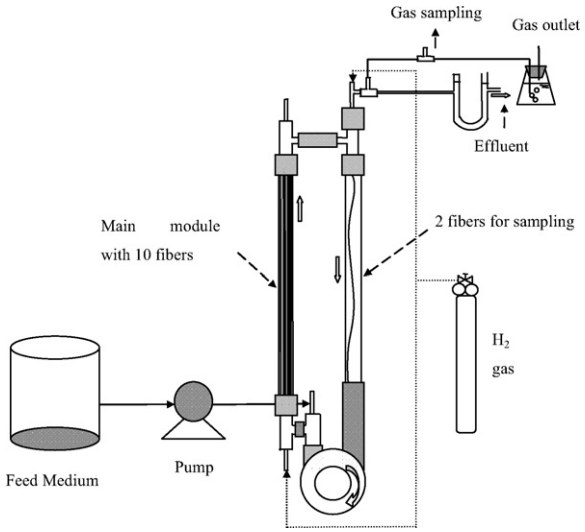

Fig. 2. Schematic of the bioreactor.

The conceptual diagram of the MBfR is shown in Fig. 1 (right). In one module, the fibers are collected in a gas supplying manifold at one end and are sealed at the opposite end (Fig. 2). The pressurized gas flows through the lumen of the fibers and diffuses through the dry pores and into the attached biofilm outside of the fiber. The contaminated fluid flow through the surface of the biofilm, within the biofilm, H_2, and NO_3^- are utilized by the hydrogenotrophic bacteria creating a driving force for mass transfer, which is favorable for nitrate reducing and H_2 utilizing. And the N_2 gas reduced by nitrate will diffuse from the bioflim to the bulk liquid.

A schematic of the laboratory scale MBfR used in this study is shown in Fig. 2. The MBfR system consisted of two membrane modules connecting to a recirculation loop. The bulk liquid in the reactor was continuously recirculated using a single peristaltic pump (Longer BT50-1J, Baoding, China) with a nitrate-medium-feed rate of 0.2–1.8 ml/min. Under the high recirculation rate (150 ml/min) and the high recirculation rate (more than 80:1), the system run was used as a completely mixed biofilm reactor to maintain a consistent biomass accumulation on the hollow fibers. The main membrane module contained a bundle of 10 hydrophobic hollow-fiber membranes inside glass pipe shell with an inner diameter 0.8 cm, and the other module contained two fibers used to collect biofilm samples. The fiber bundles have 22 cm active length to yield a specific area of 276 m^2/m^3 and provide 124 cm^2 of membrane surface area. The active volume of the bioreactor is 45 cm^3. Pure H_2 was supplied to the inside hollow fibers through the manifold at the base from a pressurized tank.

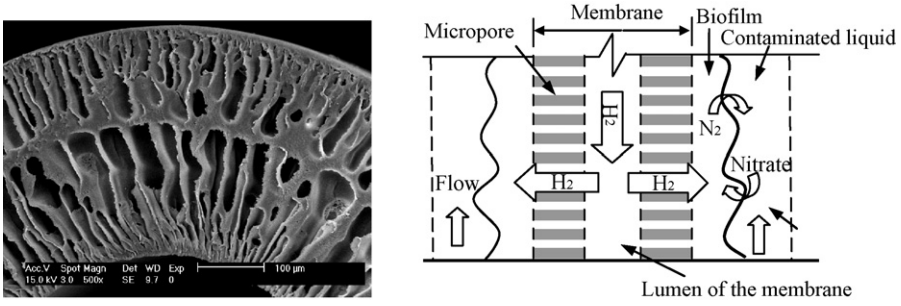

Fig. 1. Scanning electron micrograph (SEM) of cross section of the membrane (left) and the conceptual diagram of the MBfR (right).

Table 1
Experimental conditions.

	Run 1	Run 2	Run 3	Run 4	Run 5	Run 6	Run 7
Operation period (day)	1–20	21–44	45–74	75–102	103–137	138–168	260–279
HRT (min)	37.5	75.0	37.5	25.0	37.5	50.0	225.0
NO_3^-–N (mg/L)	5	5	5	5	10	10	50

2.2. Synthetic influent

In present study, the components of synthetic influent for simulating drinking water were KH_2PO_4 (0.128 g/L), Na_2HPO_4 (0.434 g/L), $MgSO_4{\cdot}7H_2O$ (0.02 g/L), $CaCl_2{\cdot}2H_2O$ (0.001 g/L), $FeSO_4{\cdot}7H_2O$ (0.001 g/L), and $NaHCO_3$ (0.252 g/L), and 1 ml trace solution, respectively. The components in 1 ml trace solution were $ZnSO_4{\cdot}7H_2O$ (100 mg/L), $MnCl_2{\cdot}4H_2O$ (30 mg/L), H_3BO_3 (300 mg/L), $CoCl_2{\cdot}6H_2O$ (200 mg/L), $CuCl_2{\cdot}2H_2O$ (10 mg/L), $NiCl_2{\cdot}2H_2O$ (10 mg/L), $Na_2MoO_4{\cdot}2H_2O$ (30 mg/L), and Na_2SeO_3 (30 mg/L), respectively. Nitrate concentration ranged from 5–50 mg NO_3^-–N/L. The synthetic influent was prepared in a 20-L glass bottle and all feed medium were purged with nitrogen gas to eliminate dissolved oxygen initially. Phosphate buffer ($KH_2PO_4 + Na_2HPO_4$) was used to keep initial pH value of the influent around 7.2 and prevent pH sharp rise in denitrification process.

2.3. Start-up and experimental conditions

Start-up of MBfR was initiated by seeding with 5 ml of anaerobic activated sludge from a municipal wastewater treatment plant in Shanghai, and the fresh influent was added glucose with final concentration of 0.5 g glucose/L for accelerating the biofilm establishing. During the start-up periods, the synthetic drinking water containing the anaerobic sludge was recirculated through MBfR for 10 days to establish a biofilm on the membrane surface under intermittent feeding fresh influent.

Then, the performance of MBfR was evaluated continuously over 168 days under the hydrogen pressure of 0.04 MPa by changing volumetric influent loading rate of nitrate, which determined by hydraulic retention time (HRT) or nitrate concentration (Table 1). Thereafter, the MBfR had been continuously operated to reduce nitrate at low influent nitrate concentrations until it was evaluated with 50 mg NO_3^-–N/L in the influent at day 260 to appreciate the viability of the technology for the project applications under the hydrogen pressure of 0.04 MPa (Table 1).

2.4. Analytical method

All the liquid samples collected from the reactor were kept in the refrigerator at 4 °C until analysis and analyzed within two days. The concentrations of NO_3^-–N, NO_2^-–N and pH value were analyzed according to Chinese NEPA standard methods [23]. The turbidity was measured using a turbidimeter (2100N, HACH, USA). Total organic carbon (TOC) analysis was performed with the Shimadzu TOC-Vcpn analyzer. The gas concentrations in the headspace of the reactor were measured by a GC 14-B quipped with a TCD detector (Shimadazu Co.). The gas sample in the headspace of the reactor was taken by inserting a gas-tight syringe through the rubber stopper on the gas-sampling port.

2.5. Scanning electron microscopy

The control membrane fibers of PVC were cleaned with distilled water and sonication for 20 min, then were dried and coated with Au/Pb for enhance the quality of the images. After the preparation, the outer surface and cross section of the fibers were examined by scanning electron microscope (SEM, XL-30, Philips, Netherlands). Biofilm samples from the reactor were taken at day 110, and these biofilm samples were checked by SEM using the same methods without the preparation of washing and sonication.

2.6. Biofilm sampling, DNA extraction, and PCR

Biofilm samples from MBfR were obtained by cutting a 4-cm-long section from the coupon fiber. The remaining fiber was sealed with a plastic wedge. The samples were collected from three periods: biofilm acclimating in Run 1 (day 10); biofilm reaching mature in Run 5 (day 110) and Run 6 (day 160), respectively.

For DNA extractions, the samples were centrifuged at 10,000 rpm for 5 min, and the DNA was extracted using a 3S DNA Isolation Kit (Shenergy color, China).

The primer pair 357f and 518r were used for amplification of the V3 region part of 16S rDNA genes [24]. A 40-nucleotide GC-rich sequence was attached to the 5′-end of the forward primers 357f to improve the detection of sequence variation in amplified DNA fragments by subsequent DGGE. Each 50 μl PCR reaction consisted of 25 ng of extracted DNA, 10 mM Tris–HCl (pH 8.3), 1 mM $MgCl_2$, 0.1 mM dNTP, 0.5 mM both primers, and 0.5 U Taq DNA polymerase (Takara, China), respectively. The PCR reactions were performed with Mycycler (Bio-Rad, USA). Amplification of the first round was run under the following conditions: initial denaturing 94 °C for 5 min followed by 30 cycles consisting of denaturation at 94 °C for 45 s, primer annealing at 58 °C for 45 s, and primer extension at 72 °C for 45 s, and a final extension step was conducted at 72 °C for 10 min.

2.7. Denaturing gel gradient electrophoresis (DGGE)

DGGE was performed using a BioRad Dcode system (Bio-Rad, USA) according to previous research [25]. The PCR products were loaded onto 8% (w/v) polyacrylamide gels in 1.0× TAE buffer. The denaturing gradient ranged from 35% to 60% denaturant. Electrophoresis was run at 200 V for 5 min firstly and then at 150 V for 5 h at 60 °C. Then, the gel was stained with SDNA-Nuleic Acids stain dye for 30 min, washed in distilled water, and finally the gel's UV transillumination image was captured using a CCD camera system.

DGGE bands were excised with a sterile knife and transferred to sterile microcentrifuge tubes. After rinsing twice with 50 μl of sterile, DI water, and eluting overnight at 4 °C, the suspended DNA was re-amplified by PCR and then DGGE was performed again as described above. After the result of the single band in one lane in DGGE was achieved, the DNA of the single band was re-amplified and sent to Sangon Company (Shanghai, China) for nucleotide sequencing. The nucleotide sequences were compared with known sequences in Genbank using the BLAST program (NCBI, USA).

2.8. Statistical analysis of DGGE banding patterns

The intensity of individual DGGE band was analyzed with Smartview (Furi Tech. Ltd., Shanghai). The diversity of microbial communities was determined using the following Shannon–Wiener index (H') to present taxa information of biofilm

from the reactor. The following equation was used:

$$\text{Shannon} - \text{wiener index}(H') = -\sum_{i=1}^{s}(p_i)(\ln p_i)$$

where s was the number of bands in the sample and p_i was the intensity proportion of sample i.

Cluster analysis was used to investigate the relationship between the microorganisms of deferent lanes in DGGE profiles, which was carried out using the NTSYS-pc (2.10, Exeter Software, USA).

2.9. Short term experiments

To systematically investigate the effect of H_2 pressure (0.02, 0.03, 0.04, 0.05, and 0.06 MPa, respectively) on autohydrogenotrophic denitrification, the short term experiments were conducted under the HRT and concentration of nitrate setting at 50 min and 10 mg N/L. For each short-term test, the system conditions lasted for 5 h before samples were taken. With a HRT of 50 min, 5 h (more than 10 HRTs) was long enough for the system and liquid concentration to reach a pseudo-steady state [26].

3. Results and discussion

3.1. Denitrification performance in MBfR

After recirculating the bulk fluent with anaerobic sludge for 10 days, the biofilm was built on the fibers. Then, the influent was fed at a rate of 1.2 ml/min (HRT = 37.5 min) to the reactor. The influent and effluent quality of MBfR was illustrated in Fig. 3. The effluent concentrations of nitrate and nitrite were about 1 and 0.2 mg N/L and about 80% of nitrate removal efficiency was accomplished after 20 days. In Run 2, HRT was changed from 37.5 to 75 min, i.e., the influent nitrate loading decreased from 192.93 ± 3.73 g N/m^3 d to 97.22 ± 2.23 g N/m^3 d, to get the better denitrification effect (Fig. 4). As we expected, the mean concentrations of nitrate and nitrite in the effluent were 0.19 and 0.08 mg N/L, respectively, and both of the nitrate and nitrite were generally not detected in the later period of this stage. As a result, the average total nitrogen removal efficiency was $94.7 \pm 6.4\%$ (Fig. 4).

The performance of Run 3 was very good, from day 45 to 74, at HRT of 37.5 min. The concentrations of nitrate and nitrite were not detected in most of time except in the beginning time of this stage (the concentrations of the effluent nitrate above 1.2 mg N/L caused by the shock of high influent nitrate loading). Correspondingly, the total nitrogen removal efficiency averaged $95.9 \pm 9.3\%$.

After 74 days, the influent nitrate loading increased gradually in Run 4 and Run 5. The performance of Run 4 was similar to Run 3, and the denitrification effect was not affected by the adding influent nitrate loading. This can be verified by that the nitrate was completely reduced without nitrite accumulation in the effluent

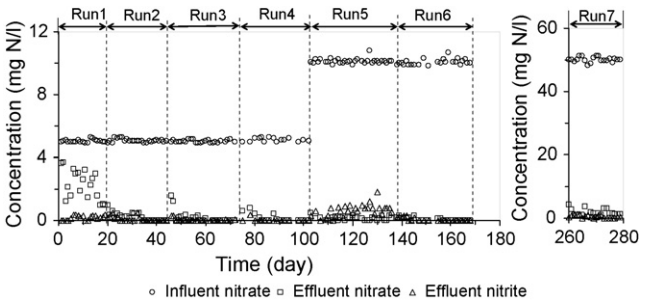

Fig. 3. The effluent concentrations of nitrate and nitrite in MBfR.

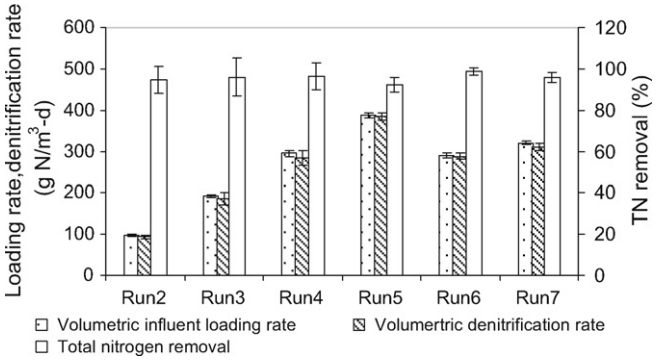

Fig. 4. Volumetric influent loading rate, volumetric denitrification rate of NO_3^-–N and total nitrogen removal at different running stages.

in most of time. However, the nitrate was not completely reduced in Run 5, with serious nitrite accumulation, for seen the average concentrations of nitrate and nitrite in the effluent were 0.13 ± 0.13 and 0.65 ± 0.37 mg N/L, respectively. This suggested that the specific denitrification rate of nitrate increased to the maximum level (1.39 g/cm^2 d) for the given hydrogen supply rate (hydrogen pressure 0.04 MPa), the cells preferentially utilized nitrate as the sink for electrons over nitrite (Fig. 5) [17]. Just for the same reason, the mean total nitrogen removal efficiencies deceased from 96.3% in Run 4 to 92.3% in Run 5. Therefore, the effluent quality of hydrogen-based autotrophic denitrification processes must be closely monitored to ensure that the nitrite concentration does not exceed regulatory level (1 mg NO_2^-–N/L in US).

In Run 6, the influent nitrate loading was decreased to a lower level (289.20 ± 5.52 g N/m^3 d) for maintaining a good effluent quality. As we expected, the total nitrogen removal efficiency during this period averaged $98.7 \pm 2.0\%$, corresponding to low concentrations of nitrate and nitrite in the effluent not more than 0.1 mg N/L.

From Run 2 to Run 5, the nitrate volumetric loading rate increased from 97.22 to 388.15 g N/m^3 d, and the volumetric denitrification rates were 93.53, 185.21, 284.74, and 383.01 g N/m^3 d, respectively, and the average TN removal efficiencies were above 92% all through the experiments. Based on the surface area of the membrane, the nitrate specific surface loading rate increased gradually from 0.35 to 1.41 g N/m^2 d, the specific denitrification rate (nitrate utilizing rate) were 0.34, 0.67, 1.03, and 1.39 g N/m^2 d, respectively. And the maximum steady-state volumetric denitrification rate achieved was 414.72 g N/m^3 d, which corresponding to a surface specific denitrifcation rate of 1.50 g N/m^2 d on day 127. And the results were favorably compared to that reported by Lee and Rittmann [14] of 1.0 g N/m^2 d and by Shin et al. [27] of 1.4 g N/m^2 d and by Visvanathan et al. [28] of 332.5 g N/m^3 d in their work with hydrogenotrophic denitrification in hollow fiber membrane bioreactors. Terada et al. [22] had reported a high surface denitrification

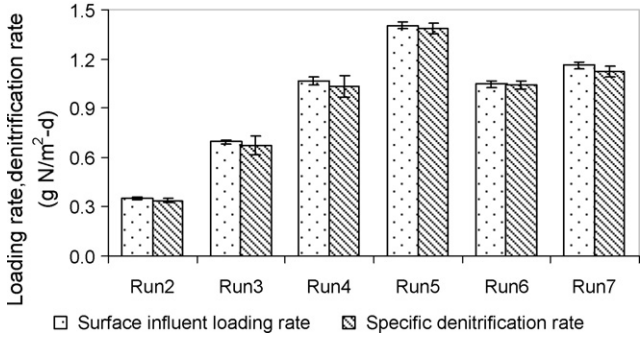

Fig. 5. Surface loading and specific denitrification rate of NO_3^-–N at different running stages.

Table 2
Water quality parameters measured in Run 6.

Parameter	Unit	Influent	Effluent
Nitrate	mg NO_3^-–N/L	10	nd
Nitrite	mg NO_2^-–N/L	nd	nd
TOC	mg C/L	2.2	3.2
DOC	mg C/L	0.3	2.0
Turbidty	NTU	0.8	4.1
Headspace H_2 content	%		3.0
Alkalinity	mg/L	513	600
pH	–	7.2	7.6

nd: not detected.

rate of 3.53–6.58 g N/m^2 d by hydrogen-based silicone membrane biofilm reactor which employing fibrous ferro-nickel slag as a bacterial carrier; however, the fabrication of gas-permeable membrane was complicated and the hydrogen utilization efficiency was lower.

During Run 7, from day 260 to day 279, the system operated at high influent nitrate concentrations of 50 ± 0.82 mg N/L and long HRT of 225 min (Fig. 3), therefore, the influent nitrate loading increased slightly compared to Run 6, for seen 320.38 g N/m^3 d (Fig. 4). As a result, the average effluent concentrations of nitrate and nitrite were 1.63 and 0.48 mg N/L, respectively, below the drinking water standard, and the total nitrogen removal efficiency was 95.8 ± 2.2%. The average volumetric denitrification rate and the average surface specific denitrifcation rate were 309.98 g N/m^3 d and 1.12 g N/m^2 d, respectively (Figs. 4 and 5). Consequently, the performance of Run 7 indicated the viability of this system to treat high nitrate concentrations in the influent.

In the last period of Run 6, the other water quality parameters in addition to NO_3^-–N and NO_2^-–N, were measured and listed in Table 2. Both of NO_3^-–N and NO_2^-–N were not detected in the effluent. Alkalinity and pH value had a clear increase due to denitrification. TOC, DOC, and turbidity analysis showed increases of 1.0 mg C/L, 1.7 mg C/L, and 3.3 NTU, respectively, most likely because the biomass was detached from the biofilm. An increase of DOC is common for autotrophic systems, since all microbial reactions are known to produce soluble microbial products (SMP) [14]. Ergas and Reuss [19] and Lee and Rittmann [14] also reported the similar results in their work with a hydrogenotrophic denitrification MBfR, the residual DOC in the effluent is easy to result in bacterial growth in the distribution system. Therefore, a further treatment, such as rapid filtration or GAC adsorption is necessary to remove biological products from the water prior to distribution. The headspace hydrogen content was 3.0%, which can be converted to liquid concentration of 49 μg/L by Henry's law at 20 °C. The results suggested that hydrogen-based MBfR using PVC hollow fiber membranes for denitrification can preclude having an explosive air, as the explosive range of hydrogen is 4–74.5%.

3.2. Microbial community structures analysis

The DGGE results were shown in Fig. 6 (right panel), with dominant band labeled with a specific number. In the steady-state stages

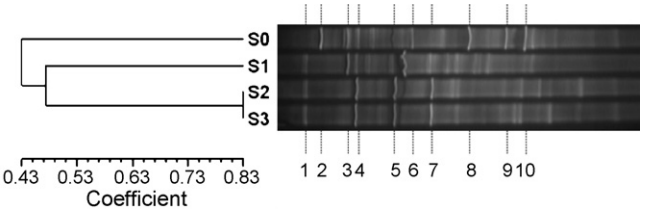

Fig. 6. Hierarchical cluster analysis of DGGE profiles demonstrated graphically as an UPGMA dendrogram (left panel) and DGGE results (right panel) for the inoculated sludge (S0), day 10 (S1), day 110 (S2), and day 160 (S3), respectively.

Table 3
Identity of dominant DGGE bands.

Band	Best Genbank match	Accession no.	Similarity
4	*Betaproteobacteria*, *Rhodocyclus*	AF314420	98%
5	*Betaproteobacteria*, *Hydrogenophaga*	AF078769	98%
7	*Betaproteobacteria*, HTCC379	AY429719	97%

of the reactor operation, the community structures were simple and dominated by several bands, which were different from that of the inoculated anaerobic sludge sample. On day 10, belonged to the acclimatizing period of hydrogenotrophic denitrifying bacteria, the dominant bands of lane decreased in Run 1 (lane S1) (only band 3, 4, 6, and 7). The main banding patterns on day 160 were similar to those on day 110, the strongest bands of the both periods were 4, 5, and 7. The results indicated that the biofilm in Run 5 and Run 6 had developed to be mature stages, and the bacterial community structures changed significantly compared to the acclimatizing stage. Also, this phenomenon could be proved by the Shannon–Wiener index values of 2.76, 2.36, 2.22, and 2.15 for the inoculated anaerobic sludge, day 10, day 110, and day 160, respectively.

The bands of DGGE were becoming simpler gradually with the time. The reasons were attributed to that the microorganisms in the inoculated sludge were adapting to the new growth environment of autotrophic, hydrogen-oxidizing, anaerobic condition, and the heterotrophic denitrifying bacteria was disappearing gradually when the new acclimating autotrophic denitrifying bacteria became dominant culture. The dominant bands on day 110 and day 160 with numbers of 4, 5, and 7 were excised and sequenced (Table 3). They were similar to *Rhodocyclus* (similarity 98%), *Hydrogenophaga* (similarity 98%), and *beta-Proteobacteria* HTCC379 (similarity 97%), respectively. All of the three microorganisms belong to beta divisions within the *Proteobacteria*. Stephanie et al. [29] also found that the clones and the extinction cultures obtained by extinction culture techniques were both dominated by representatives of the *beta-Proteobacteria* in the bioremediation in trichloroethene contaminated groundwater. The *Hydrogenophaga* and *beta-Proteobacteria* HTCC379 were also found in their studies. Numbers of *Hydrogenophaga* are chemo-organotrophic or chemolithoautotrophic, using the oxidation of H_2 as an energy source and CO_2 as a carbon source [30]. However, HTCC379 was not identified for utilizing H_2 to reduce nitrate in the ground water. *Rhodocyclales* sp. HOD 5, a strain of purple non-sulfur photosynthetic, had been found in nitrate-contaminated ground water earlier and had been proved to be able to grow aerobically on hydrogen to remove oxygen and nitrate [31–33]. Therefore, the *beta-Proteobacteria*, which including *Rhodocyclus*, *Hydrogenophaga*, and *beta-Proteobacteria* HTCC379 (Table 3), probably play a major role in denitrification of MBfR.

Hierarchical cluster analysis was used to demonstrate similarities in the banding profiles of samples. The results were presented in the form of UPGMA dendrograms (Fig. 6, left panel). The community structure of the inoculated anaerobic sludge had lower similarity to those of the day 10, day 110, and day 160, with the similarity coefficient of 43.5%, 39.1%, and 47.8%, respectively. However, a high similarity was found between day 110 and day 160 with a coefficient of 82.6%, indicating that their communities were homogenous relativity and no major transitions occurred.

3.3. Electron microscopic analysis of the contract membrane and biofilm in MBfR

The surface morphologies of the control hollow fiber and biofilm surface from the reactor were shown in Fig. 7. The outer surface of the control fiber showed the surface structure of the PVC hollow fiber was flat; however, the micro-pores of 0.01 μm could not

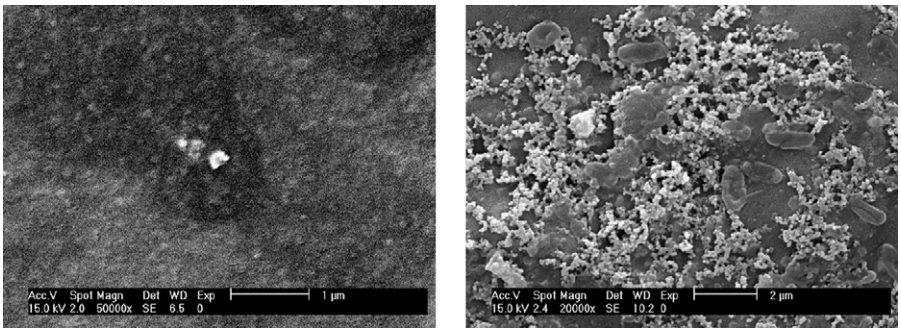

Fig. 7. Scanning electron micrograph of surface (left) of control fiber and scanning electron micrograph of bioflim from MBfR (right).

be seen clearly because of special process for film fabrication. The biofilm taken from the reactor consisted of individual rod-shape bacteria about 0.5 μm in diameter and 2 μm long.

3.4. Short-term experiments results

Short-term experiments were carried out to further investigate the hydrogen pressure effect on denitrification at fixed influent nitrate surface loading of 1.04 g/m^2 d, and the results were shown in Fig. 8. Nitrate concentrations decreased as the hydrogen pressure increased from 0.02 to 0.04 MPa sharply, and then declined slowly from hydrogen pressure 0.04 to 0.06 MPa (Fig. 8 panel a). However, residual nitrite concentrations were higher at low hydrogen pressure (0.8, and 1.08 mg N/L at 0.02, and 0.03 MPa, respectively), and were very low at hydrogen pressure from 0.04 to 0.06 MPa.

This trend suggested that the accumulation of nitrite was associated with hydrogen pressure at fixed influent nitrate loading [14]. Correspondingly, the percentage removals of TN (i.e., NO_3^-–N + NO_2^-–N) and nitrate were above 90% at the hydrogen pressure above 0.04 MPa, and the TN removals were very low at hydrogen pressure below 0.04 MPa (Fig. 8 panel b).

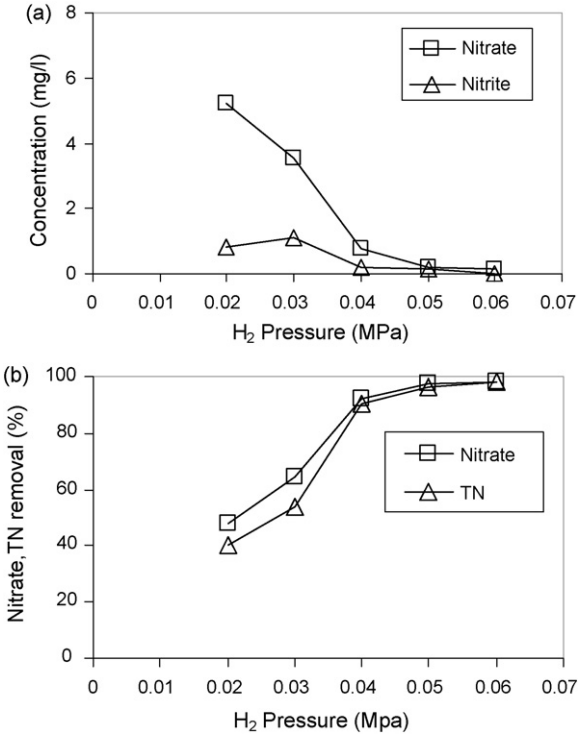

Fig. 8. Nitrate and nitrite concentrations in effluent (panel a) and total nitrogen and nitrate removals (panel b) at different hydrogen pressure.

4. Conclusions

A PVC hollow fiber MBfR successfully established an autohydrogenotrohic denitrifying biofilm to remove nitrate using H_2 as electron donor. The PVC hollow fiber has an inner diameter of 0.085 cm, an outer diameter of 0.15 cm and a 0.01 μm pore size. During the 279-day operation period, the maximum denitrification rate reached a maximum value of 414.72 g N/m^3 d at an influent NO_3^-–N concentration of 10 mg/L and a hydraulic residence time of 37.5 min, and the influent nitrates were completely reduced. The maximum surface denitrification rate of 1.50 g N/m^2 d was achieved, which was favorably compared to composite membranes based on analysis of cost-benefit. In addition, the experiment also indicated the viability of this system to treat high nitrate concentrations in the influent.

While, the effluent quality analysis showed the headspace hydrogen contents were lower enough to preclude having explosive air. DOC analysis suggested that the residual DOC in the effluent is easy to result in bacterial growth in the distribution system. Therefore, a further treatment, such as rapid filtration or GAC adsorption is necessary to remove biological products from the water prior to distribution.

Electron microscopic analysis clearly showed the section structure of the contract membrane, and confirmed the shape and size of the autohydrogenotrophic denitrifiers on the biofilm. Under the influent nitrate surface loading of 1.04 g/m^2 d, over 90% removals of TN and nitrate were achieved at the hydrogen pressure above 0.04 MPa. The removals of TN and nitrate were relatively low at hydrogen pressure lower than 0.04 MPa.

The results of DGGE showed that the microbial community structures in the mature stage had a low diversity that was stable in autohydrogenotrophic denitrification biofilm [33]. The 16S rDNA gene sequence analysis and hierarchical cluster analysis showed that microbial community structures of two mature stages in MBfR were homogenous relativity and no major transitions occurred, and the *beta-Proteobacteria*, including *Rhodocyclus*, *Hydrogenophaga*, and *beta-Proteobacteria* HTCC379, probably play an important role in autohydrogenotrophic denitrification.

Acknowledgements

The authors thank to the Programs of Internationally Scientific Cooperation (2007DFB90280, 2007DFR90050) and Special Program of World Exposition (07DZ05814) for providing the financial support.

References

[1] M. Shrimali, K.P. Singh, New methods of nitrate removal from water, Environ. Pollut. 112 (2001) 351–359.
[2] M.I.M. Soares, Biological denitrification of groundwater, Water Air Soil Pollut. 123 (2000) 183–193.

[3] WHO, Guidelines for Drinking Water Quality, 3rd ed., Geneva, 2003.
[4] D.C. Bouchard, M.K. Williams, R.Y. Surampalli, Nitrate contamination of groundwater: sources and potential health effects, Am. Water Works Assoc. 84 (1992) 85–90.
[5] B.U. Bae, Y.H. Jung, W.W. Han, H.S. Shin, Improved brine recycling during nitrate removal using ion exchange, Water Res. 36 (2002) 3330–3340.
[6] J.J. Schoeman, A. Steyn, Nitrate removal with reverse osmosis in a rural area in South Africa, Desalination 155 (2003) 15–26.
[7] J.W. Peel, K.J. Reddy, B.P. Sullivan, J.M. Bowen, Electrocatalytic reduction of nitrate in water, Water Res. 37 (2003) 2512–2519.
[8] M.A. Gomez, E. Hontoria, J. Gonzalez-Lopez, Effect of dissolved oxygen concentration on nitrate removal from groundwater using a denitrifying submerged filter, J. Hazard. Mater. 90 (2002) 267–278.
[9] J.M. Flere, T.C. Zhang, Sulfur-based autotrophic denitrification pond systems for in-situ remediation of nitrate-contaminated surface water, Water Sci. Technol. 38 (1998) 15–22.
[10] J.M. Flere, T.C. Zhang, Nitrate removal with sulfur-limestone autotrophic denitrification processes, J. Environ. Eng.: Asce 125 (1999) 721–729.
[11] A. Koenig, T. Zhang, L.-H. Liu, H.H.P. Fang, Microbial community and biochemistry process in autosulfurotrophic denitrifying biofilm, Chemosphere 58 (2005) 1041–1047.
[12] D. Dries, J. Liessens, W. Verstraete, P. Stevens, P. de Vos, J. de Ley, Nitrate removal from drinking water by means of hydrogenotrophic denitrifiers in a polyurethane carrier reactor, Water Supply 6 (1988) 181–192.
[13] M. Kurt, J. Dunn, J.R. Bourne, Biological denitrification of drinking water using autotrophic organisms with H_2 in a fluidized-bed biofilm reactor, Biotechnol. Bioeng. 29 (1987) 493–501.
[14] K.C. Lee, B.E. Rittmann, A novel hollow fiber membrane biofilm reactor for autohydrogenotrophic denitrification of drinking water, Water Sci. Technol. 41 (2000) 219–226.
[15] S.M. Hee, W.C. Sun, N. Kyoungphile, Effect of reactive media composition and co-contaminants onsulfur-based autotrophic denitrification, Environ. Pollut. 144 (2006) 802–807.
[16] R. Sierra-Alvarez, R. Beristain-Cardoso, M. Salazar, J. Gomez, E. Razo-Flores, J.A. Field, Chemolithotrophic denitrification with elemental sulfur for groundwater treatment, Water Res. 41 (2007) 1253–1262.
[17] K.C. Lee, B.E. Rittmann, Applying a novel autohydrogenotrophic hollow-fiber membrane biofilm reactor for denitrification of drinking water, Water Res. 36 (2002) 2040–2052.
[18] B.E. Rittmann, Hydrogen-based membrane-bioreactor solves oxidized contaminated problems, Membrane Technol. 2002 (2002) 6–10.
[19] S.J. Ergas, A.F. Reuss, Hydrogenotrophic denitrification of drinking water using a hollow fibre membrane bioreactor, Water Supply Res. Technol. AQUA 50 (2001) 161–171.
[20] A. Kapoor, T. Viraraghavan, Nitrate removal from drinking water - Review, Journal of Environmental Engineering-Asce 123 (1997) 371–380.
[21] K.S. Haugen, M.J. Semmens, P.J. Novak, A novel in situ technology for the treatment of nitrate contaminated groundwater, Water Res. 36 (2002) 3497–3506.
[22] A. Terada, S. Kaku, S. Matsumoto, S. Tsuneda, Rapid autohydrogenotrophic denitrification by a membrane biofilm reactor equipped with a fibrous support around a gas-permeable membrane, Biochem. Eng. 31 (2006) 84–91.
[23] NEPA, Water and Wastewater Monitoring Methods, third ed., Chinese Environmental Science Publishing House, Beijing, China, 1997.
[24] B.K. Mobarry, M. Wagner, V. Urbain, B.E. Rittmann, D.A. Stahl, Phylogenetic probes for analyzing abundance and spatial organization of nitrifying bacteria, Appl. Environ. Microbiol. 62 (1996) 2156–2162.
[25] S.Q. Xia, J.F. Guo, R.C. Wang, Performance of a pilot-scale submerged membrane bioreactor (MBR) in treating bathing wastewater, Bioresour. Technol. 99 (2008) 6834–6843.
[26] J. Chung, R. Nerenberg, B.E. Rittmann, Bio-reduction of soluble chromate using a hydrogen-based membrane biofilm reactor, Water Res. 40 (2006) 1634–1642.
[27] J.H. Shin, B.I. Sang, Y.C. Chung, Y.K. Choung, A novel CSTR-type of hollow fiber membrane biofilm reactor for consecutive nitrification and denitrification, Desalination 221 (2008) 526–533.
[28] C. Visvanathan, N.Q. Hung, V. Jegatheesan, Hydrogenotrophic denitrification of synthetic aquaculture wastewater using membrane bioreactor, Process Biochem. 43 (2008) 673–682.
[29] A.C. Stephanie, T. Adisorn, D. Mark, V. Kevin, J.G. Stephen, Bacterial community composition determined by culture-independent and -dependent methods during propane-stimulated bioremediation in trichloroethenecontaminated groundwater, Environ. Microbiol. 7 (2005) 165–178.
[30] K. Peter, S. Renate, J. Udo, A.M. Khursheed, A. Rudolf, S. Stefan, *Hydrogenophaga defluvii* sp. nov. And *Hydrogenophaga atypica* sp. nov., isolated from activated sludge, Int. J. Syst. Evol. Microbiol. 55 (2005) 341–344.
[31] R.L. Smith, M.L. Ceazan, M.H. Brooks, Autotrophic, hydrogen-oxidizing, denitrifying bacteria in groundwater, potential agents for bioremediation of nitrate contamination, Appl. Environ. Microbiol. 60 (1994) 1949–1955.
[32] R.L. Smith, S.P. Buckwalter, D.A. Repert, D.N. Miller, Small-scale, hydrogen-oxidizing-denitrifying bioreactor for treatment of nitrate-contaminated drinking water, Water Res. 39 (2005) 2014–2023.
[33] R. Nerenberg, Y. Kawagoshi, B.E. Rittmann, Microbial ecology of a perchlorate-reducing, hydrogen-based membrane biofilm reactor, Water Res. 42 (2008) 1151–1159.